P4.17 ANALYSIS OF FLAT CONVECTION DURING THE MORNING BOUNDARY-LAYER TRANSITION USING AIRBORNE MEASUREMENTS

Thomas Spieß, Peter Zittel, and Jens Bange

Aerospace Systems at Technical University Braunschweig, Germany

1. INTRODUCTION

The transition of the nocturnal stable boundary layer to a convective boundary layer (CBL) is not very well understood compared to other topics like processes within the daytime CBL (Wayne et al., 2001). A few experimental investigations were already made. E.g. Lenschow et al. (1979) found that during this transition the wind, temperature, and humidity vary with the terrain. But in general little is know about the flat convection in the early morning shallow boundary layer. The present paper deals with the investigation of flat convection during the morning transition using data of the helicopter-borne turbulence probe Helipod. The data of four flights on four different days during a LITFASS-Experiment (**L**indenberg **I**nhomogeneous **T**errain - **F**luxes between **A**tmosphere and **S**urface: a Long-Term **S**tudy, Beyrich *et al.* 2002) in 2002 were analyzed in different terms of scaling.

2. MEASUREMENT SYSTEMS

The Helipod (Fig. 1) is a unique measurement system of about 5 m in length, 0.5 m in diameter, and 250 kg in weight. It is an autonomously operating sensor package constructed to be carried by almost any helicopter on a rope of 15 m length. At a typical ground speed of 40 ms^{-1} (Fig. 2) the Helipod is outside the downwash area of the rotor blades. It carries its own navigation systems, power supply, data storage, and fast responding sensor equipment. The system was especially designed for in situ measurements of the turbulent fluctuations of wind, temperature, humidity, and the turbulent fluxes (e.g., Bange *et al.*, 2002; Bange and Roth, 1999).

To achieve a high temporal resolution, the Helipod measures each meteorological parameter with at least two different types of instruments: One that has a short response time, but the disadvantage of a temporal drift, is sampled at 100 Hz. The other type responds slowly but is very accurate on a large time scale, and is sampled at 20 Hz. To achieve a large frequency range, the data sets are combined by complementary filters. The results are 100 Hz time series of the meteorological parameters, equivalent to one measurement point every 40 cm. Due to its

Fig. 1: *The helicopter-borne turbulence probe Helipod*

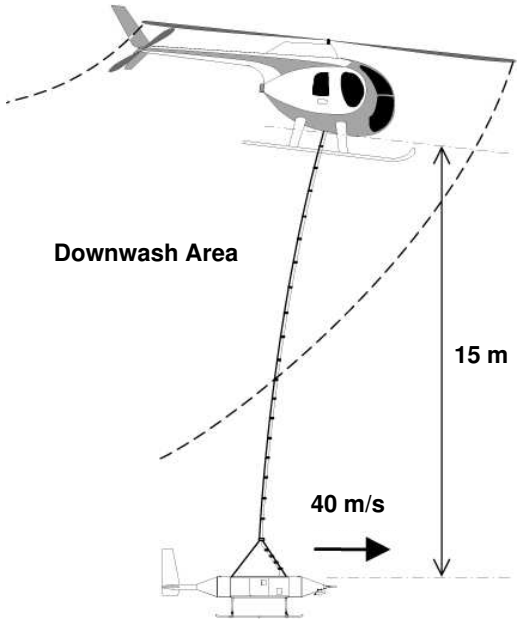

Fig. 2: *The principle of the Helipod flight: At a true airspeed of 40 ms^{-1} the system is out of the downwash area.*

Corresponding author: Thomas Spieß, Aerospace Systems, Technical University of Braunschweig, Germany; e-mail: t.spiess@tu-bs.de

small fuselage, and the absence of wings and propulsion the influence of the Helipod on the atmosphere is small compared to conventional research aircrafts. Additionally the Helipod is no subject to approval (FAA, JAA) and is in general allowed to perform lower and slower flights than an airplane.

3. EXPERIMENT AND FLIGHT PATTERN

The Helipod performed 40 hours of measurement flights during the STINHO-2 (**ST**ructure of the turbulent transport over **INHO**mogeneous surfaces) experiment in 2002 which was embedded into the framework of the LITFASS experiments (Spieß *et al.*, 2003; Spieß *et al.*, 2004). In this measurement campaign many other groups were involved. Seven micro-meteorological stations were installed on different surface types, mostly on bare soil or grassland. Furthermore, four laser scintillometers, a long-distance scintillometer, a 99 m meteorological tower, a wind profiler/RASS system (Engelbart and Bange, 2002), a SODAR, a differential absorption LIDAR (DIAL) system (Bösenberg and Linné, 2002), an acoustic tomography system (Raabe *et al.*, 2004), and other systems performed simultaneous measurements.
One of the goals of this sub-campaign was the comparison of Helipod data with Large-Eddie Simulations (LES) and the acoustic tomography. On four days in the very early morning flight measurements were performed during the boundary-layer transition. The Helipod performed a grid flight pattern called 'Small Grid' which consisted of 12 straight legs of 5 km length, 6 of them oriented in north-south direction, the other 6 legs in west-east direction (Fig. 3). The center of the flight pattern was the 99 m tower of the German Weather Service at 14^{o}07'27" E and 52^{o}10'01" N at a field elevation of 73 m above mean sea level (msl). The flights were performed at a constant low altitude. Furthermore, vertical sounding were produced using slant flights at several locations.

4. WEATHER CONDITIONS

The flights took place in the early morning of the 5, 6, 8, and 9 July, 2002. On Friday 5 July the flight took place in good conditions after the passage of a cold front associated with a low-pressure system centered over Jutland.

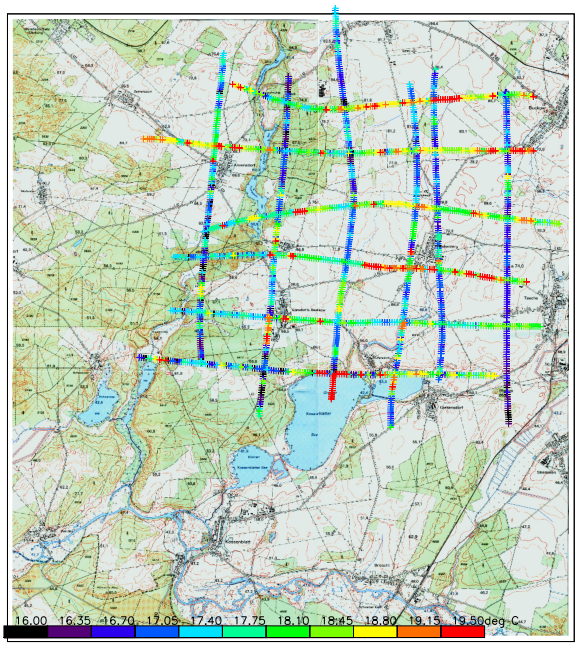

Fig. 3: *The Helipod flight pattern 'Small Grid'. The color of the line is the measured surface temperature.*

During the measurements between 5.00 and 6.45 UTC the sky was clear which were good conditions for evolving flat convection. In the morning of the next day 3/8 high cirrus clouds were observed during the flight. A new trough of low pressure was approaching from the west which caused more and more clouds during the day and some rain in the evening. The 6 July was the only one where the complete measurement flight (5.00 - 6.45 UTC) was in stable or slightly stable conditions which is shown in figure 4. Because of bad flight weather there was no flight on Sunday, 7 July but the next day the measurement area had high pressure influence and no clouds so there were good conditions for data acquisition which took place between 5.15 and 7.00 UTC. Figure 5 shows several vertical soundings of this morning. The transition from the stable nocturnal boundary layer to a convective boundary layer with rising boundary layer hight is visible. On 9 July, 2002 the last day of the measurements the high pressure influence was decreasing. During the flight in the early morning only 1/8 cirrus clouds were observed. Figures 6 and 7 show the general weather situation on 6 and 8 July, 2002.

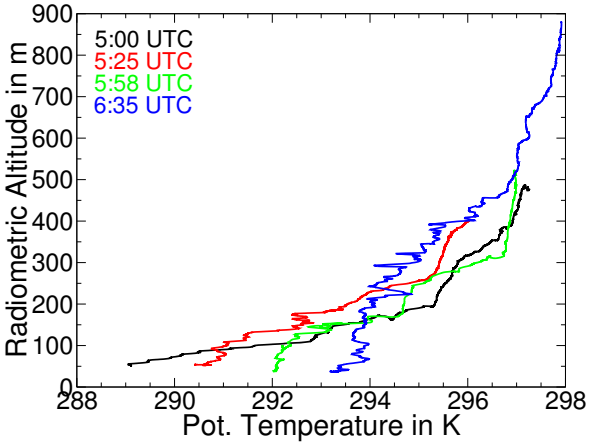

Fig. 4: *Vertical profiles of the potential temperature on 6 July, 2002. The lines were smoothed with a moving average over 8 seconds.*

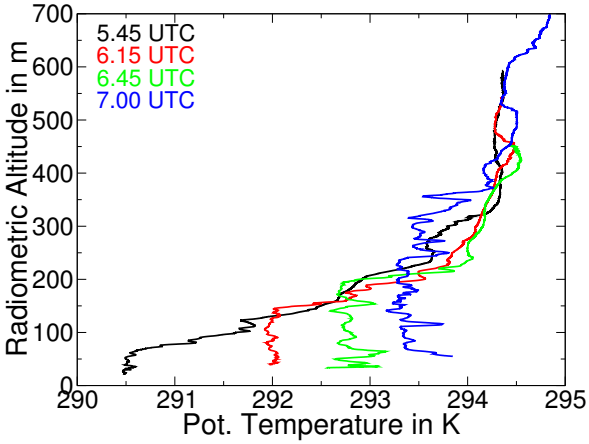

Fig. 5: *Vertical profiles of the potential temperature on 8 July, 2002. The lines were smoothed with a moving average over 8 seconds.*

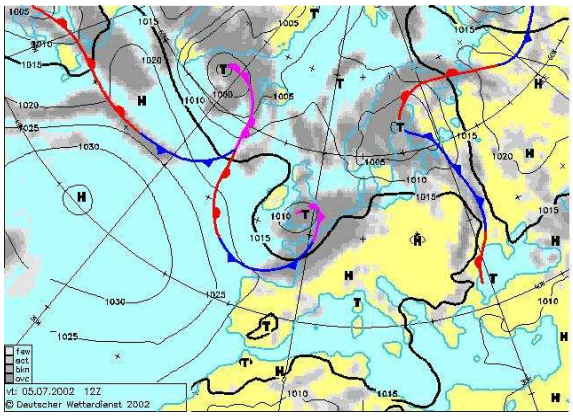

Fig. 6: *General weather situation on 6 July, 2002*

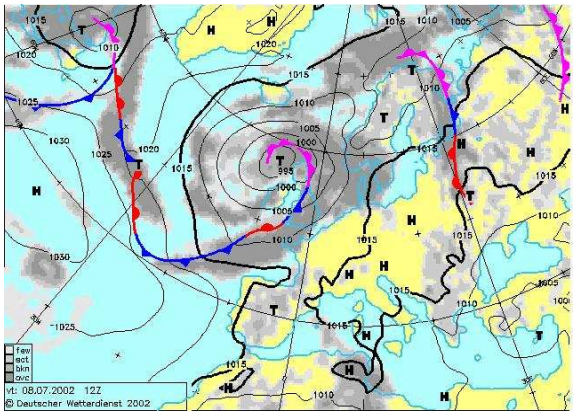

Fig. 7: *General weather situation on 8 July, 2002*

5. DATA SETS AND METHODS

The collected Helipod data of all four 'Small Grid' flights in the early morning was analyzed. Within the frame of this paper the presentation of the results is restricted to the flights on 6, 8, and 9 July, 2002. The measurements on 6 July were in stable and slightly stable conditions and the development of the 8 July (neutral stratification) is comparable to 5 and 9 July.

During all flights the Helipod flew at a constant flight level z of about 80 m above ground. The rising CBL gave the opportunity to an unusual vertical profiling of the atmospheric boundary layer (ABL): Not the measurement platform was moving vertically but the boundary layer height z_i. So each leg of the grid flight pattern had a different value of z/z_i. It is not known to the author that vertical profiles in terms of z/z_i-scaling were performed in the same way with an airborne measurement system before.

There had been lots of experiments with towers, e.g. the 200 m tower at Cabauw, the Netherlands (e.g., Driedonks, 1982; Angevine *et al.*, 2001) but tower measurements mostly require other systems to get data for altitudes higher than the tower height. Mast measurements always depend on the fetch so the advantage of airborne measurements is the possibility to cover a larger area. For the analysis of 6 July, 2002 the local scaling theory (Nieuwstadt, 1984) was applied because of the stable stratification conditions. Nieuwstadt introduced a so called 'local Obukhov length' Λ

$$\Lambda = -\frac{\tau^{3/2}}{\kappa(g/T)\langle w'\theta'\rangle}\,. \qquad (1)$$

which is based on the Obukhov length. In (1)

$\tau = [\langle w'u' \rangle^2 + \langle w'v' \rangle^2]^{1/2}$ is the momentum flux, κ is the von Karman constant taken equal to 0.35 (Nieuwstadt, 1984), g/T is the buoyancy parameter, and $\langle w'\theta' \rangle$ is the vertical sensible heat flux divided by the air density ρ and the heat capacity c_p. The brackets identify the average over an entire flight leg in this study.

6. RESULTS

Figure 8 shows the standard deviations of the wind velocities non-dimensionalized with the local momentum flux τ as a function of z/Λ. The best fit curves of the standard deviations are linear which is equal to Nieuwstadt (1984) and Caughey, Wyngaard, and Kaimal (1979) who also made a linear fit. For $z \cdot \Lambda^{-1} < 1$ the standard deviation of the vertical wind component $\sigma_w/\tau^{1/2}$ is in the same order around 1.7. But in contrast to the articles the standard deviations rise for $z \cdot \Lambda^{-1} > 1$ which means that the locally scaled standard deviations do not become z-less. This result is comparable to Kroonenberg, Spieß, and Bange (2004) but must be reviewed critically considering the low number of available data sets.

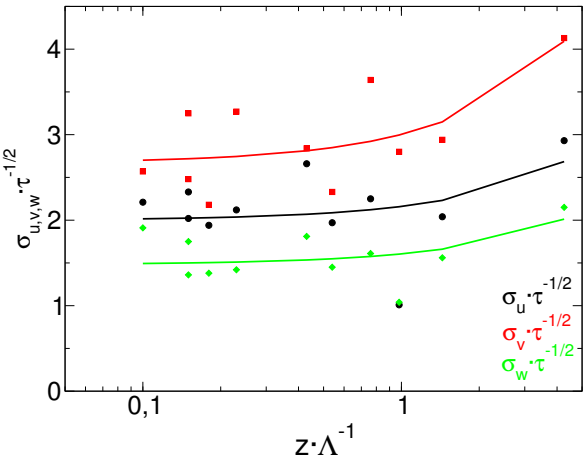

Fig. 8: *Local scaled, nondimensionalized standard deviations of the wind components on 6 July, 2002*

Figure 9 shows the sensible heat flux as a function of z/Λ. As expected the value of the heat flux increased as z/Λ decreased.

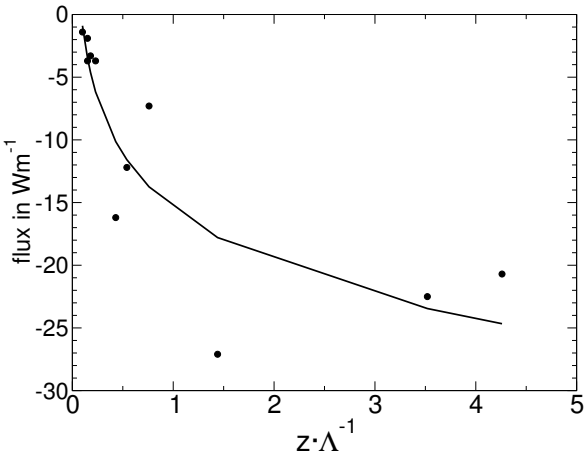

Fig. 9: *Local scaled sensible heat flux on 6 July, 2002*

Lenschow, Stankov, and Mahrt (1979) found large spatial differences of the potential temperature, the humidity, and wind speed over slight terrain inhomogeneities during the morning transition after the begin of surface heating. These differences were found as well in the vertical soundings of this study.
Within figure 4 the temporal evolution of the potential temperature is visible. It is possible to identify several different layers with different stabilities in the sounding at 5.25 UTC and 5.58 UTC which is also shown in figure 10. Figure 11 shows the horizontal wind speed. The maximum of the low-level jet (LLJ) at 180 m corresponds to the step in the temperature profile shown in figure 10. The transition from the stable nocturnal boundary layer to the residual layer can be observed in both profiles at 300 m height.

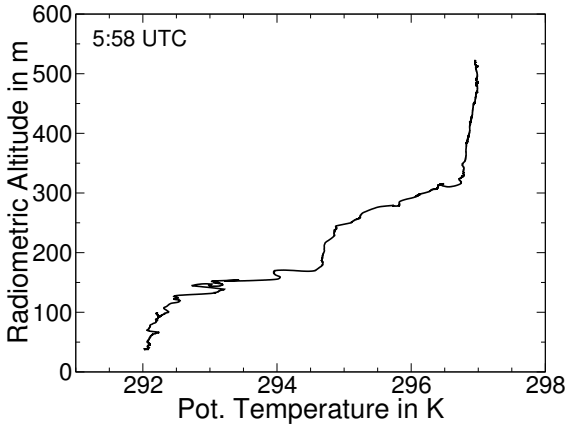

Fig. 10: *Vertical profile of the potential temperature on 6 July, 2002. The line was smoothed with a moving average over 8 seconds.*

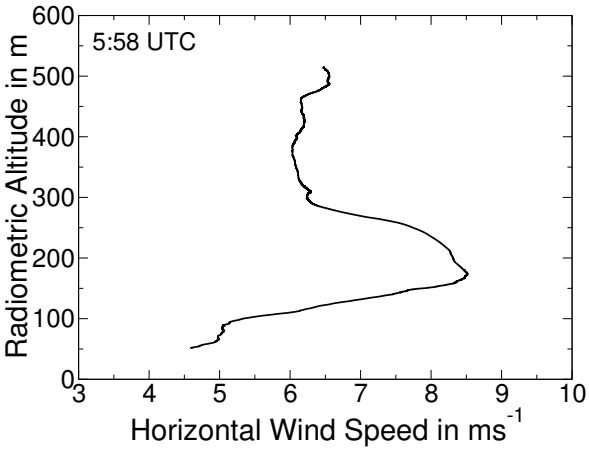

Fig. 11: *Vertical profile of the horizontal wind speed on 6 July, 2002. The line was smoothed with a moving average over 8 seconds.*

Figure 12 shows the profile of the wind speed of a different vertical sounding. The black line is the ascend of the profile, the red line is the descend. Because there was no turn or change in the flight direction between the ascend and descend the profiles had hardly any temporal but only a spatial separation of just a few kilometers. Although the low level jet is visible in the ascend (black line) it nearly disappeared in the descent (red line). Furthermore the difference of about 3 ms^{-1} in the value of the wind speed near the ground indicates the spatial variability caused by the inhomogeneities of the surface.
These are interesting observations that will be investigated more detailed in the future.

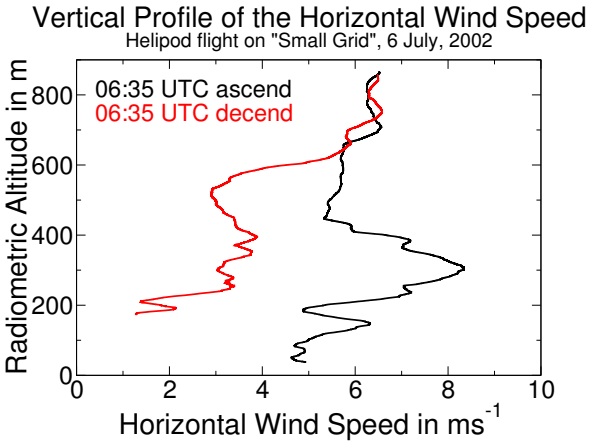

Fig. 12: *Vertical profile of the horizontal wind speed at 6.35 UTC on 06. July, 2002. The line was smoothed with a moving average over 8 seconds.*

For the analysis of the other three days the z/z_i scaling (e.g., Deardorff, 1970) was applied. During a complete flight the altitude of the legs ranged between a normalized height of z/z_i = 0.25 and $z/z_i \gg 1.0$. For the present investigation all legs with $z/z_i < 1.0$ were included. One of the results for the 8 July, 2002, which are in general also transferable to the 5 and 9 July is shown in figure 13. Each point corresponds to the vertical sensible heat flux calculated from a single leg. The best fit line is comparable to a typical profile in a daytime convective boundary layer of the sensible heat flux as it can be found in the literature, modeled by numerical simulations (e.g. LES) or found with measurements (e.g., Stull, 1988; Hechtel *et al.*, 1990). This shows that the flat convection during the morning transition behaves like the convection of an evolved daytime CBL. The 15 legs of figure 13 with $z/z_i < 1.0$ were flown between 5.57 UTC and 7.00 UTC so all the legs were inside the flat convection. The interpolation of the sensible heat flux with the best fit line led to a value of about 102 Wm^{-2} at the ground. The corresponding time to this value is around 6.28 UTC. The value of a long distance scintillometer (LAS) with a path of several kilometers and a 10 minute mean was 94 Wm^{-2} at 6.30 UTC. For the other two days the surface values of the LAS and the interpolation of the Helipod values led to good agreement as well. The LAS was the most suitable measurement system for the comparison with the Helipod because it also measured over a mixture of surfaces (forest, bare soil, grassland, wheat fields, corn fields, etc.).

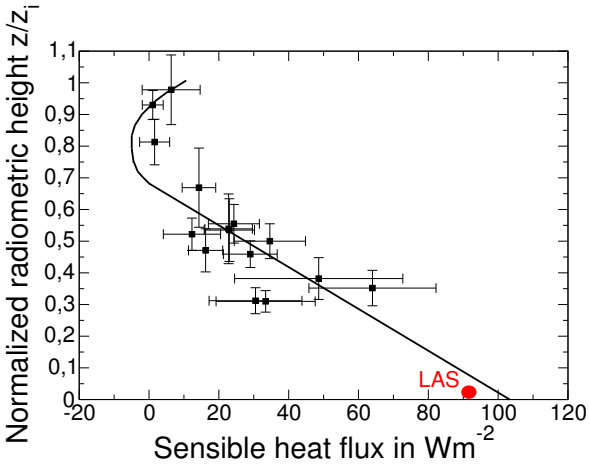

Fig. 13: *z/z_i-scaled sensible heat flux on 8 July, 2002. The linear interpolation of the Helipod values to the ground ($z/z_i < 0.7$) fits to the LAS value. The curve for $z/z_i > 0.7$ is fitted by eye.*

It seems to be appropriate to make a linear interpolation of the single legs to the ground although the conditions during the morning change rapidly. It is assumed that this is just possible because the measurements were made before the very rapid growth phase of the CBL. However the effect of the instationarity of the atmosphere has to be studied more detailed.

It is also remarkable that the Helipod and LAS measurements were close to each other although the error of the flux calculation is quite large due to the short length of the legs. The statistical errors of the flight measurements were calculated according to **?**) with improvements by Zittel, Spieß, and Bange (2004). There was no information about the statistical error of the LAS.

Again the vertical profiles of the 8 July, 2002 were analyzed. Figures 14 - 17 show the vertical profiles of the potential temperature, the water vapor mixing ratio, the wind speed, and the wind direction. In general the atmosphere at 5.45 UTC was stably stratified for altitudes higher than 150 m above ground. This is no contradiction to figure 13 because there it was later and the Helipod flew at a lower altitude so that the evolved flat convection in neutral stratification had crossed the flight level. The potential temperature had two significant ramps at a height of about 290 m and 380 m above ground measured with a radio altimeter. At the same height the humidity exhibits huge changes so different layers can be identified. This becomes more clearly with a look at the wind profiles. A low level jet in the wind speed is visible and the wind direction shows a strong wind shear in the region between 290 m and 380 m. This wind shear caused some turbulence which can be identified in the fluctuations of the potential temperature between 340 m and 380 m and must be intermittent turbulence due to the stable stratification. Time series of the wind compounds (not shown) reveal the intermittent character of these turbulent events.

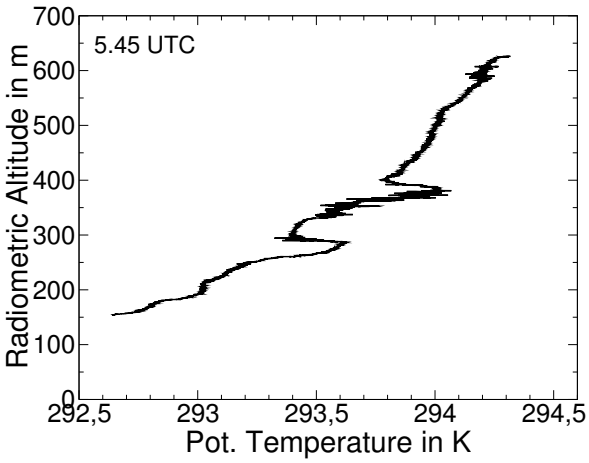

Fig. 14: *Vertical profile of the potential temperature on 8 July, 2002.*

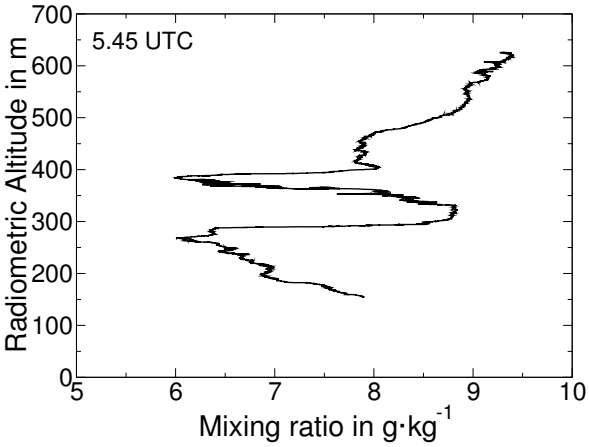

Fig. 15: *Vertical profile of the water vapor mixing ratio on 8 July, 2002.*

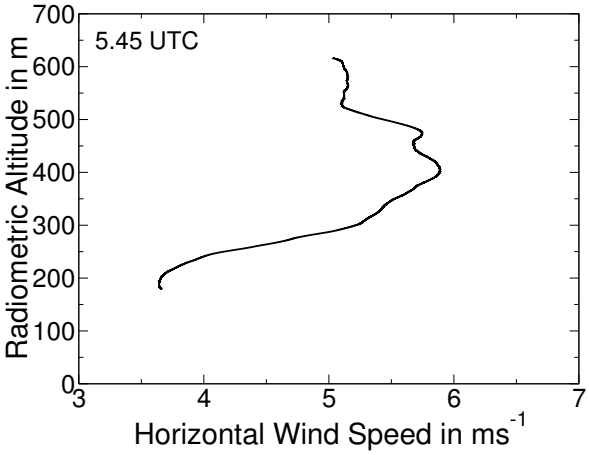

Fig. 16: *Vertical profile of the horizontal wind speed on 8 July, 2002. The line was smoothed with a moving average over 8 seconds.*

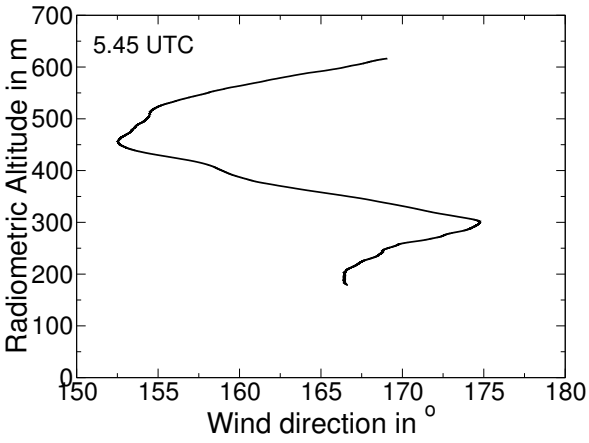

Fig. 17: *Vertical profile of the wind direction on 8 July, 2002. The line was smoothed with a moving average over 8 seconds.*

Another vertical sounding of the 8 July, 2002 is shown in figures 18 and 19. This profile was flown at about 07.00 UTC and shows two significant ramps in the potential temperature and in the moisture. Between 437 m and 440 m the potential temperature rose and dropped again more than 1 K which led to a gradient of $\Gamma > 33$ Kelvin per 100 m. In the same region between 437 m and 440 m the humidity changed more than 2.3 g/kg which led to more than 80 g/kg per 100 m (see figures 20 and 21).

The temperature, humidity, and wind measurement of the Helipod were independent from each other. The sensors were located at different positions with different power supplies. Therefore, a malfunction in the measurement equipment can be excluded. The analysis is not yet completed but the observed small scaled ramps and their gradients are the largest ever measured with an airborne system. Evidence of very thin layers of (relative) cold and moist air has been reported before (e.g., Muschinski and Wode, 1998) but the observed gradients on 8 July, 2002 were much larger.

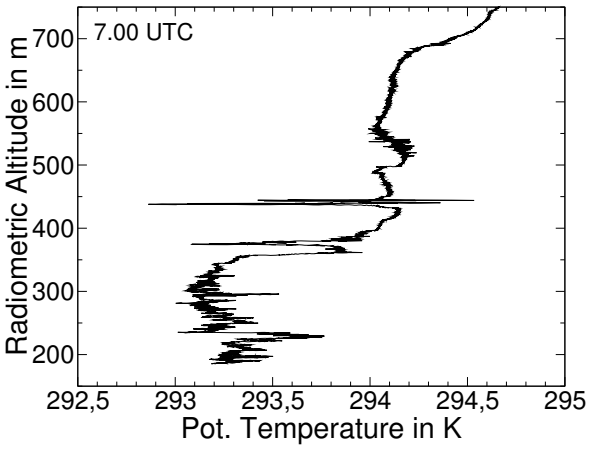

Fig. 18: *Vertical profile of the potential temperature at 07.00 UTC on 8 July, 2002.*

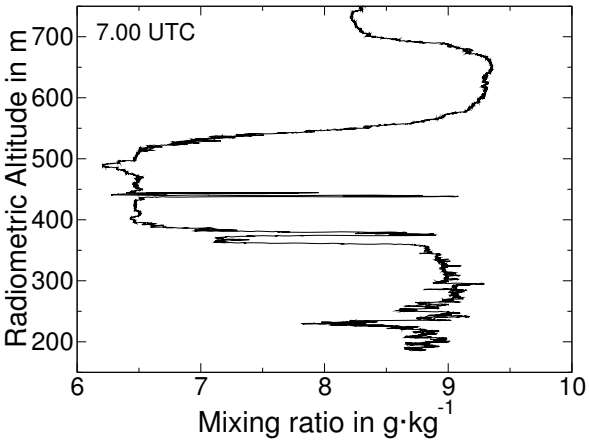

Fig. 19: *Vertical profile of the mixing ratio at 07.00 UTC on 8 July, 2002.*

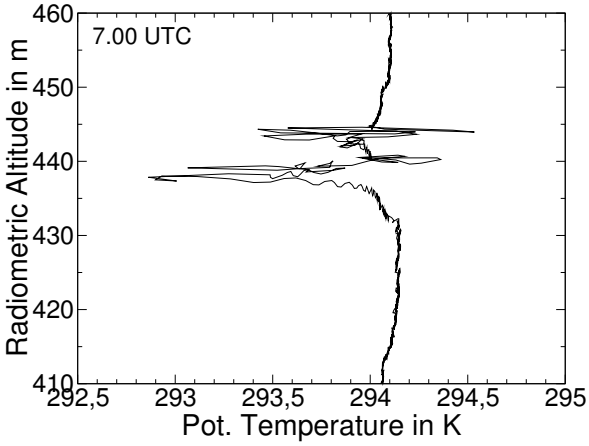

Fig. 20: *Detailed look into the vertical profile of the potential temperature at 07.00 UTC on 8 July, 2002.*

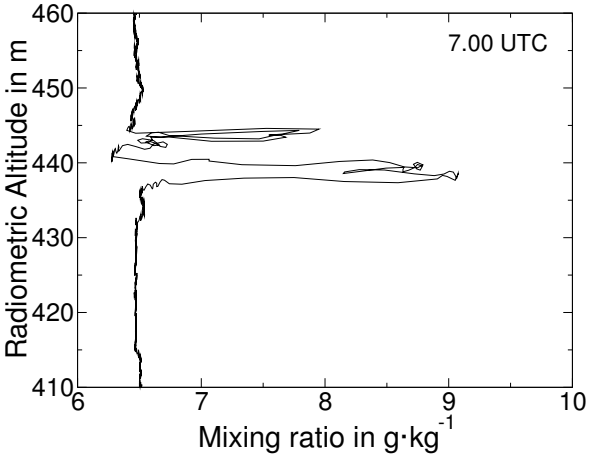

Fig. 21: *Detailed look into the vertical profile of the mixing ratio at 07.00 UTC on 8 July, 2002.*

6. OUTLOOK

There are still lots of observations and data sets that should be analyzed. E.g. the standard deviations of the wind compounds of the three unstable stratified days can be analyzed and compared with other investigations (e.g., Mangesha *et al.*, 2001).

The latent fluxes will be analyzed and should be compared with other measurements such as remote sensing systems.

More experiments are required for a better data base. Numerical models have problems simulating the transition of the stable boundary layer to a convective boundary layer because of the small scale of the involved processes. Because many phenomenons are sub-scaled, parameterizations are used. The experimental study of the transition will help to find solutions for the parameterizations, which can be used by the sub-grid calculations of numerical models.

Especially for high resolved airborne measurements in stable conditions the Helipod already received a complete upgrade that will be finished in autumn 2004. The main computer is being replaced by a single board computer with commercial industry components, temperature proof to -30^{o}C (PowerPC, MEN Company, Nürnberg, Germany). A real-time operating system of the Unix family, 'Real-Time Linux', controls the commercial input-/output modules. The modernized Helipod has 32 differential A/D-channels, an ARINC interface for the LITEF inertial navigation system, three GPS receivers and antennas for complete attitude alignment (Septentrion Company), and a flash-storage. The choice of industry hardware components saved money and will make updates easier. The recording rate will increase to 500 Hz with an anti-aliasing low-pass filter at 100 Hz, and an oversampling of at least 3 kHz for noise reduction. This will increase the unmuted spatial resolution to 40 cm, which is in the order of the diameter of the Helipod. This will be the highest spatial resolution of an airborne system by now. Instead of the former online data processing the data is post processed for better complementary or Kalman filtering especially of the navigation data. Furthermore, new measurement equipment will be integrated, such as CO_2 sensors, ozone sensors, infrared- and optical cameras, etc.

ACKNOWLEDGMENT

We are much obliged to the crew of the FJS Helicopter Service in Damme (Germany) who performed the flights with the Helipod. The Helipod flights and the field experiments were funded by the German government (BMBF: EVA-GRIPS within DEKLIM, grant no. 01-LD-0301 and VERTIKO within AFO2000, grant no. 07-ATF-37).

REFERENCES

Angevine, W., **H. Baltink**, and **F. Bosveld**, **2001**: Observations of the Morning Transition of the Convectice Boundary Layer. *Boundary-Layer Meteorol.*, **101**, 209 – 227.

Bange, J., **F. Beyrich**, and **D. A. M. Engelbart**, **2002**: Airborne Measurements of Turbulent Fluxes during LITFASS-98: A Case Study about Method and Significance. *Theor. Appl. Climatol.*, **73**, 35–51.

Bange, J. and **R. Roth**, **1999**: Helicopter-Borne Flux Measurements in the Nocturnal Boundary Layer Over Land - a Case Study. *Boundary-Layer Meteorol.*, **92**, 295–325.

Beyrich, F., **H.-J. Herzog**, and **J. Neisser**, **2002**: The LITFASS Project of DWD and the LITFASS-98 Experiment: The Project Strategy and the Experimental Setup. *Theor. Appl. Climatol.*, **73**, 3–18.

Bösenberg, J. and **H. Linné**, **2002**: Laser Remote Sensing of the Planetary Boundary Layer. *Meteorol. Z.*, **11**, 233–240.

Caughey, S. J., **J. C. Wyngaard**, and **J. C. Kaimal**, **1979**: Turbulence in the Envolving Stable Boundary Layer. *J. Atmos. Sci.*, **36**, 1041–1052.

Deardorff, J., **1970**: Convective Velocity and Temperature Scales for the Unstable Planetary Boundary Layer and for Rayleigh Convection. *J. Atmos. Sci.*, **27**, 1211–1213.

Driedonks, A., **1982**: Models and Observations of the Growth of the Atmospheric Boundary Layer. *Boundary-Layer Meteorol.*, **23**, 283–306.

Engelbart, D. A. M. and **J. Bange**, **2002**: Determination of Boundary-Layer Parameters using Wind Profiler/RASS and Sodar/RASS in the Frame of the LITFASS-Project. *Theor. Appl. Climatol.*, **73**, 53–65.

Hechtel, L. M., **C.-H. Moeng**, and **R. B. Stull**, **1990**: The Effects of Nonhomogeneous Surface Fluxes on the Convective Boundary Layer: A Case Study Using Large-Eddy Simulation. *J. Atmos. Sci.*, **47**, 1721–1741.

Kroonenberg, A. C. v. d., **T. Spieß**, and **J. Bange**, **2004**: Observation of Intermittent Turbulence over Artic Sea-Ice. In: *16th Symposium on Boundary Layers and Turbulence*, AMS, Portland/Maine, USA. 4.7.

Mangesha, Y., **P. Taylor**, and **D. Lenschow**, **2001**: Boundary-Layer Turbulence Over the Nebraska Sandhills. *Boundary-Layer Meteorol.*, **100**, 3 – 46.

Muschinski, A. and **C. Wode**, **1998**: First In-Situ Evidence for Co-Existing Sub-Meter Temperature and Humidity Sheets in the Lower Free Troposphere. *J. Atmos. Sci.*, **55**, 2893–2906.

Nieuwstadt, F., **1984**: The Turbulent Structure of the Stable, Nocturnal Boundary Layer. *J. Atmos. Sci.*, **41**, 2202–2216.

Raabe, A., **K. Arnold**, **A. Ziemann**, **M. Schröter**, **S. Raasch**, **J. Bange**, **P. Zittel**, **T. Spieß**, **T. Foken**, **M. Göckede**, **F. Beyrich**, and **J.-P. Leps**, **2004**: STINHO - STructure of turbulent transport under INHOmogeneous surface conditions - a micro-α scale field experiment and LES modelling. *Met. Zeitschr.*. Submitted.

Spieß T., **P. Zittel**, and **J. Bange**, **2003**: Helipod Measurements during VERTIKO and EVAGRIPS Campaigns in 2002. In: *EGS-EGU-EUG Joint Assembly*, EGU, Nice, France.

Spieß T., **P. Zittel**, and **J. Bange**, **2004**: The role of the helicopter-borne turbulence probe Helipod in joint field campaigns. In: *AMS: Eighth Symposium on Integrated Observing and Assimilation Systems for Atmosphere, Oceans, and Land Surface*, AMS, Seattle, USA. P7.6.

Stull, R., **1988**: *Boundary Layer Meteorology*. Kluver Acad., Dordrecht, 666 pp.

Zittel, P., **T. Spieß**, and **J. Bange**, **2004**: The calculation of the statistical error of measured turbulent fluxes - considerations and improvement. In: *AMS: 17th Conference on Probability and Statistics in the Atmospheric Sciences*, AMS, Seattle, USA. 6.7.